Bioorganic & Medicinal Chemistry 22 (2014) 5270–5278

Contents lists available at ScienceDirect

Bioorganic & Medicinal Chemistry

journal homepage: www.elsevier.com/locate/bmc

Synthesis and evaluation of a ^{18}F-labeled spirocyclic piperidine derivative as promising σ_1 receptor imaging agent

Yuan-Yuan Chen [a], Xia Wang [a], Jin-Ming Zhang [b], Winnie Deuther-Conrad [c], Xiao-Jun Zhang [b], Yiyun Huang [d], Yan Li [a], Jia-Jun Ye [a], Meng-Chao Cui [a], Jörg Steinbach [c], Peter Brust [c], Bo-Li Liu [a], Hong-Mei Jia [a,*]

[a] Key Laboratory of Radiopharmaceuticals (Beijing Normal University), Ministry of Education, College of Chemistry, Beijing Normal University, Beijing 100875, China
[b] Nuclear Medicine Department, Chinese PLA General Hospital, Beijing 100853, China
[c] Helmholtz-Zentrum Dresden-Rossendorf, Institute of Radiopharmaceutical Cancer Research, Department of Neuroradiopharmaceuticals, 04318 Leipzig, Germany
[d] PET Center, Department of Diagnostic Radiology, Yale University School of Medicine, New Haven, CT, USA

ARTICLE INFO

Article history:
Received 16 April 2014
Revised 18 July 2014
Accepted 5 August 2014
Available online 12 August 2014

Keywords:
PET
^{18}F
Sigma-1 receptors
Imaging agent
Spirocyclic piperidine derivatives

ABSTRACT

Several spirocyclic piperidine derivatives were designed and synthesized as σ_1 receptor ligands. In vitro competition binding assays showed that the fluoroalkoxy analogues with small substituents possessed high affinity towards σ_1 receptors and subtype selectivity. Particularly for ligand 1′-((6-(2-fluoroethoxy)pyridin-3-yl)methyl)-3*H*-spiro[2-benzofuran-1,4′-piperidine] (**2**), high σ_1 receptor affinity (K_i = 2.30 nM) and high σ_1/σ_2 subtype selectivity (142-fold) as well as high σ_1/VAChT selectivity (234-fold) were observed. [^{18}F]**2** was synthesized using an efficient one-pot, two-step reaction method in a home-made automated synthesis module, with an overall isolated radiochemical yield of 8–10%, a radiochemical purity of higher than 99%, and specific activity of 56–78 GBq/μmol. Biodistribution studies of [^{18}F]**2** in ICR mice indicated high initial brain uptake and a relatively fast washout. Administration of haloperidol, compound **1** and different concentrations of SA4503 (3, 5, or 10 μmol/kg) 5 min prior to injection of [^{18}F]**2** significantly decreased the accumulation of radiotracer in organs known to contain σ_1 receptors. Ex vivo autoradiography in Sprague–Dawley rats demonstrated high accumulation of radiotracer in brain areas with high expression of σ_1 receptors. These encouraging results prove that [^{18}F]**2** is a suitable candidate for σ_1 receptor imaging with PET in humans.

1. Introduction

Sigma-1 (σ_1) receptors are intracellular transmembrane proteins, consisting of 223 amino acids and assumed to possess two transmembrane domains.[1,2] They function as 'ligand-operated receptor chaperones' and serve as an inter-organelle signaling modulator locally at the mitochondrion-associated endoplasmic reticulum (ER) membrane (MAM) and remotely at the plasma membrane.[3,4] Increasing evidence suggests that σ_1 receptors interact with pharmacologically different drugs and are involved in various human diseases including, in particular, protein conformation diseases.[4] In the central nervous system (CNS), σ_1 receptors regulate a variety of signal transduction processes, ER stress, cellular redox, cellular survival, and synaptogenesis,[5–7] and are thus implicated in anxiety, depression, schizophrenia, drug addiction, Alzheimer's disease, and neuroinflammation.[5–8] Moreover, they have also been shown to be involved in cardiovascular disease[9,10] and in the development of human tumors,[11,12] especially those with positive progesterone receptor status.[13] Therefore, the σ_1 receptor represents a potential target for both diagnosis and therapeutic development of a wide range of diseases.

The noninvasive imaging of σ_1 receptors by positron emission tomography (PET) has potential not only to provide an innovative pharmacological approach for the diagnosis of diseases but also to contribute to a better understanding of the physiological and pathophysiological role of σ_1 receptors.[14] However, only a few radiotracers such as [^{11}C]SA4503,[15–17] [^{18}F]FPS[18] and [^{123}I]TPCNE[19] (Fig. 1) have been evaluated in humans until now. Among these, [^{18}F]FPS[20] and [^{123}I]TPCNE[19] were found to have irreversible kinetics in humans. SA4503 showed affinity for the vesicular acetylcholine transporter (VAChT) (K_i = 50.2 nM),[21] although [^{11}C]SA4503 did not seem to bind to VAChT in the rat brain in vivo.[22] In addition, clinical use of [^{11}C]SA4503 needs an on-site cyclotron. More recently, [^{18}F]fluspidine[23] and [^{18}F]FTC-146[24,25](Fig. 1) have been shown to be promising PET radiotracers for visualizing σ_1

* Corresponding author. Tel./fax: +86 10 58808891.
E-mail address: hmjia@bnu.edu.cn (H.-M. Jia).

http://dx.doi.org/10.1016/j.bmc.2014.08.003
0968-0896/

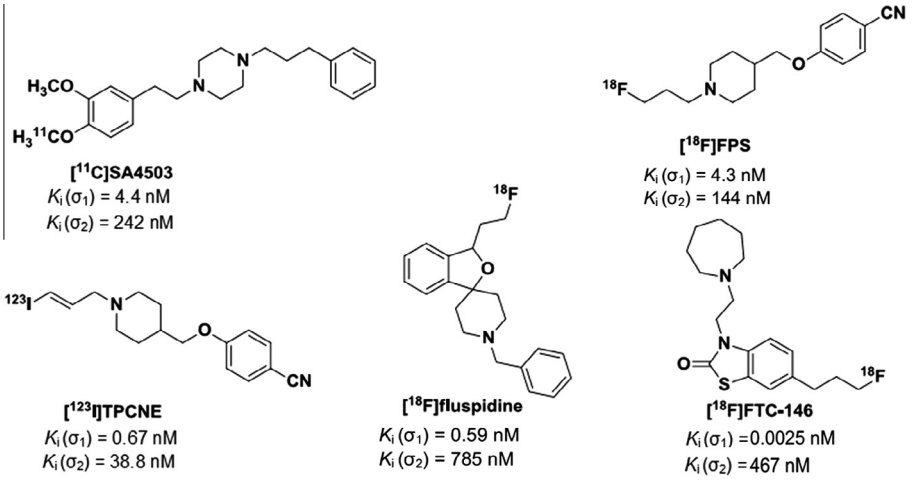

Figure 1. The structures of potential σ_1 receptor radiotracers.

receptors, but their prospects for eventual clinical translation require further investigation. Therefore, there is still need for the development of radiotracers with appropriate affinity and high specificity for σ_1 receptors to accurately quantify σ_1 receptors and provide useful diagnostic tools for investigation of diseases related to σ_1 receptors.

In the past decade, a novel class of spirocyclic piperidine compounds were reported as potent σ_1 receptor ligands and used as lead compounds to develop radiotracers for σ_1 receptor imaging.[23,26–28] In our previous work,[29] we have found that [^{18}F]1′-(4-(2-fluoroethoxy)benzyl)-3*H*-spiro[2-benzofuran-1,4′-piperidine] ([^{18}F]**1**) is a promising σ_1 receptor imaging agent with subnanomolar affinity for σ_1 receptors (K_i = 0.79 nM) and excellent σ_1/σ_2 subtype selectivity (350-fold), as well as high σ_1/VAChT selectivity (799-fold). This radiotracer displayed high initial brain uptake and high accumulation in brain areas known to express high levels of σ_1 receptors. However, its clearance rate was very slow in the brain. In order to avoid irreversible kinetics and find radiotracers with relatively fast washout rate in the brain, we modified the *N*-benzyl group and designed analogs of spirocyclic piperidine as shown in Figure 2. It was previously reported that replacement of the aromatic ring with a pyridine at the *N*-benzyl moiety only slightly decreased the affinity for σ_1 receptors.[29] Moreover, such modification could lower the lipophilicity and accordingly decrease the non-specific binding in vivo. In an attempt to modify the affinity and pharmacokinetic properties, we added a carbon atom at the *para*-substituent of the *N*-benzyl group to investigate the effects of an elongation of the fluoroalkoxy group as well as the effects of the position of the oxygen atoms. Herein we report on the synthesis and evaluation of the above spirocyclic piperidine derivatives as σ_1 receptor ligands in vitro. In addition, we labeled the previously reported ligand 1′-((6-(2-fluoroethoxy)pyridin-3-yl)methyl)-3*H*-spiro[2-benzofuran-1,4′-piperidine] (**2**) with ^{18}F and evaluated the potential of [^{18}F]**2** as a putative σ_1 receptor imaging agent in vivo.

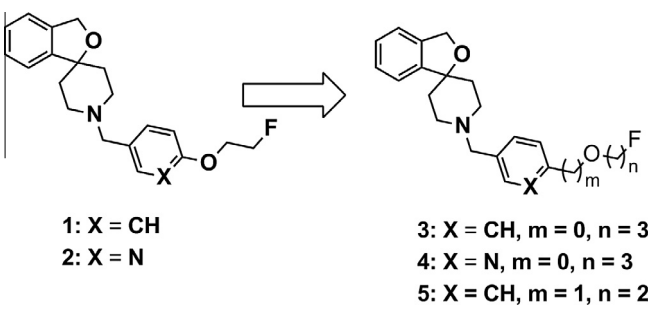

Figure 2. Design concept of spirocyclic piperidine derivatives.

2. Results and discussion

2.1. Organic chemistry

The synthetic routes of spirocyclic piperidine derivatives are showed in Scheme 1. The intermediates **6**, **7**, **8**, **9** and **10** were synthesized based on the methods reported in the literature.[29–31] Compound **2** was synthesized according to the method reported previously.[29] Reductive amination of compound **8** in the presence of $NaBH(OAc)_3$ with 4-(hydroxymethyl)benzaldehyde led to compound **11**. Reaction of intermediate **9** or **10** with 3-fluoropropyl 4-methylbenzenesulfonate (**7**) under basic condition (K_2CO_3) in acetonitrile provided compound **3** or **4** in 61% or 33% yield, respectively. Intermediate **11** reacted with 1-bromo-2-fluoroethane in acetone at 60 °C to give compound **5** in 32% yield. The target compounds (**3**, **4** and **5**) were characterized and shown to have >95% purity.

2.2. Radiochemistry

We employed an efficient one-pot, two-step reaction method to synthesize [^{18}F]**2** with a home-made automated synthesis module. The synthetic routes towards [^{18}F]**2** are outlined in Scheme 2. In the first step, ethane-1,2-diyl bis(4-methylbenzenesulfonate) **12** reacted with dried Kryptofix 2.2.2/K^+/[^{18}F]F^- complex in acetonitrile at 90 °C to provide 2-[^{18}F]fluoroethyl-1-tosylate **13**. The desired radiotracer [^{18}F]**2** was obtained via alkylation reaction between the precursor **10** and **13** in the presence of NaOH for 20 min at 110 °C. After cooling to room temperature, the mixture was passed through a C18 Sep-Pak cartridge to remove inorganic salts including [^{18}F]KF. The crude product was eluted and purified by an isocratic semi-preparative radio-HPLC using a reverse-phase column and a mobile phase consisting of acetonitrile and water (containing 10 mM NH_4OAc) (40:60, v/v) at a flow rate of 4 mL/min. Retention time of [^{18}F]**2** was 33.4 min (Fig. S1, Supplementary data). The radioactive peak corresponding to [^{18}F]**2** was collected, diluted with water and passed across a C18 Sep-Pak cartridge. The cartridge was washed with water. The product was eluted off with ethanol and diluted with sterile saline to provide a solution with approximately 370 kBq of radioactivity per 0.1 mL.

In order to identify the radiotracer, [^{18}F]**2** and reference compound **2** were co-injected and their HPLC profiles assessed using

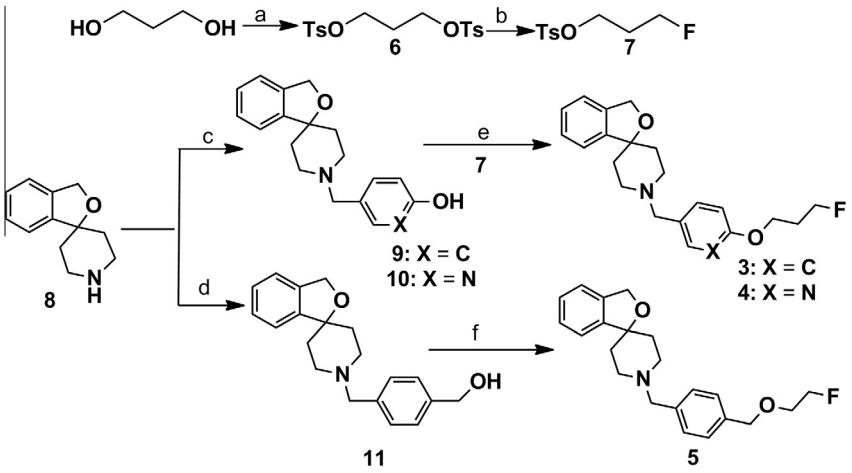

Scheme 1. Synthetic routes of spirocyclic piperidine derivatives. Regents and conditions: (a) TsCl, KOH, CH_2Cl_2, 0 °C, 83%; (b) TBAF (1 mol/L in THF), CH_3CN, reflux, 41%; (c) for **9**, (i) 4-hydroxybenzaldehyde, 1,2-dichloroethane, 2 h; (ii) $NaBH(OAc)_3$, 6 h, 69%; for **10**, (i) 6-hydroxynicotinaldehyde, 1,2-dichloroethane, 2 h; (ii) $NaBH(OAc)_3$, 24 h, 24%; (d) (i) 4-(hydroxymethyl)benzaldehyde, 1,2-dichloroethane, 2 h, (ii) $NaBH(OAc)_3$, 48 h, 33%; (e) **7**, CH_3CN, K_2CO_3, reflux, 61% for **3**, 33% for **4**; (f) 1-bromo-2-fluoroethane, K_2CO_3, acetone, 60 °C, 10 h, 32%.

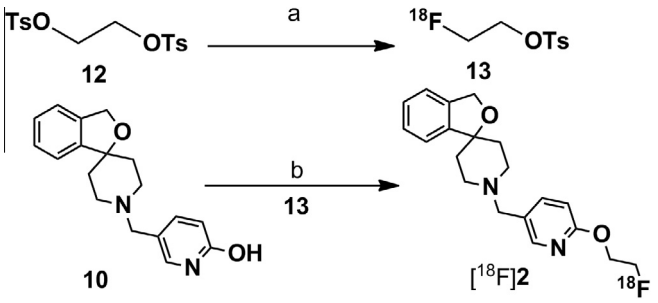

Scheme 2. Synthesis of the radiotracer [^{18}F]**2**. Reagents and conditions: (a) Kryptofix 2.2.2, K_2CO_3, CH_3CN, 90 °C, 15 min; (b) **13**, 2 mol/L NaOH, DMSO, 110 °C, 20 min.

acetonitrile and water (containing 10 mM NH_4OAc) (60:40, v/v) as mobile phase at a flow rate of 1 mL/min are presented in Figure 3. The retention times of **2** and [^{18}F]**2** were observed to be 10.88 and 10.97 min, respectively. The difference in retention times was in accordance with the time lag due to the volume and flow rate within the distance between the UV and radioactivity detectors

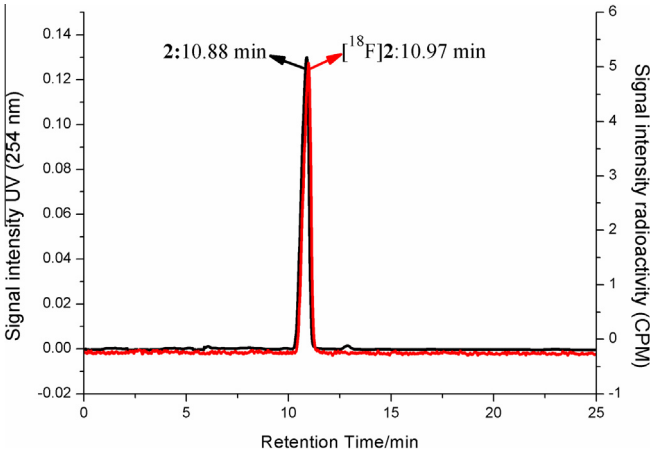

Figure 3. HPLC co-elution profiles of **2** and [^{18}F]**2**, with retention time of 10.88 and 10.97 min, respectively. Conditions: CH_3CN/H_2O (containing 10 mM NH_4OAc) = 60/40, v/v, flow rate = 1 mL/min.

of our HPLC system. After purification by semi-preparative radio-HPLC, the radiochemical purity (RCP) of [^{18}F]**2** was higher than 99%. The overall isolated radiochemical yield was 8–10% ($n = 3$, corrected for decay). The total synthesis time was about 1 h. The specific activity was 56–78 GBq/μmol.

The in vitro stability of [^{18}F]**2** in mouse plasma was evaluated by measuring the RCP at different time points. After 2 h and 4 h of incubation with mouse plasma at 37 °C, the RCP of [^{18}F]**2** was 96% and 95%, respectively (Fig. S2, Supplementary data), suggesting high stability of [^{18}F]**2** in vitro.

Lipophilicity in terms of the apparent distribution coefficient at pH 7.4 was determined by shake-flask method in a 1-octanol and 0.05 mol/L potassium phosphate buffer system. The log*D* value of [^{18}F]**2** was determined to be 2.58 ± 0.01 ($n = 3$), which is within the range expected to have good blood–brain barrier permeability. In addition, the retention times of unlabeled **1** and **2** using acetonitrile and water (containing 10 mM NH_4OAc) (60:40, v/v) as mobile phase at a flow rate of 1 mL/min were 10.32 and 10.18 min, respectively (Fig. S3, Supplementary data). These data indicate that the lipophilicity of [^{18}F]**2** is slightly lower than that of [^{18}F]**1**, which is in good agreement with our expectation that replacement of a benzene ring with pyridine decreases the lipophilicity of the compound.

2.3. Biological studies

2.3.1. In vitro radioligand competition studies

The competition binding assays for σ_1 and σ_2 receptors were carried out as previously reported.[32] The σ_1 and σ_2 receptor affinities of the new compounds were determined with the radioligands (+)-[^{3}H]pentazocine and [^{3}H]DTG (in the presence of 10 μM dextrallorphan) using rat brain and rat liver membranes, respectively. The K_i values of the compounds are listed in Table 1. Replacement of the benzene ring with pyridine decreased the affinity for σ_1 receptors slightly (**1** vs **2**, **3** vs **4**). Substitution at para-position of the benzyl moiety with increased chain length also led to decreased σ_1 receptor affinity (**1** vs **3**). Moreover, the position of the oxygen atom in the substituent at the para-position of the benzyl moiety has much influence on the σ_1 receptor affinity. Replacement of the $OCH_2CH_2CH_2F$ with a $CH_2OCH_2CH_2F$ group dramatically decreased the σ_1 receptor affinity (**3** vs **5**).

In addition, the affinities of compound **2** for VAChT were also determined in radioligand competition experiments as previously

Table 1
Binding affinities of the spirocyclic piperidine derivatives towards σ_1 and σ_2 receptors[a]

Compound	K_i (σ_1) (nM)	K_i (σ_2) (nM)	K_i (σ_2)/K_i (σ_1)
1[b]	0.79 ± 0.11	277 ± 71	350
2[b]	2.30 ± 0.69	327 ± 47	142
3	3.32 ± 0.71	143 ± 11	43
4	4.00 ± 1.14	131 ± 8	33
5	57.5 ± 3.6	2803 ± 202	49
Haloperidol	4.95 ± 1.74	20.7 ± 0.07	4

[a] Values are means ± SD of three experiments performed in triplicate.
[b] From Ref. 29.

reported.[33] Compound **2** displayed low affinity for VAChT (K_i = 538 ± 14 nM) and was thus characterized by an excellent selectivity for σ_1 receptors (K_i(VAChT)/K_i(σ_1) = 234).

Considering compound **2** possesses nanomolar affinity for σ_1 receptors and high selectivity for σ_2 receptors and VAChT as well as the lowest lipophilicity within this series, it was selected for ^{18}F-labeling and [^{18}F]**2** evaluated for its potential as σ_1 receptor radiotracer.

2.3.2. Biodistribution and blocking studies in male ICR mice

In order to evaluate the pharmacokinetics of [^{18}F]**2**, we performed in vivo biodistribution studies in male ICR mice. Experimental data are summarized in Table 2. [^{18}F]**2** showed a high initial brain uptake with radioactivity concentration of 8.39 ± 1.54% ID/g at 2 min post-injection (p.i.). The accumulation in the brain was highest at 15 min p.i. (8.56 ± 0.34% ID/g), and slowly decreased thereafter with 6.61 ± 1.22% ID/g at 30 min, 4.62 ± 0.17% ID/g at 60 min, and 3.31 ± 0.33% ID/g at 120 min. Since [^{123}I]TPCNE suffers from irreversible binding in the human brain,[19] a radiotracer with less avid binding to σ_1 receptors was suggested to be better suited for clinical applications. In our previous work, the accumulation of [^{18}F]**1** in the brain was found to be highest at 30 min p.i. with 9.32 ± 0.50% ID/g, and decreased very slowly to 8.99 ± 0.37% ID/g at 120 min p.i.[29] Replacement of the benzene ring in [^{18}F]**1** with a pyridine resulted in [^{18}F]**2** with about 3 times lower affinity (0.79 vs 2.30 nM for **1** and **2**, respectively) and lower lipophilicity (The retention times of unlabeled **1** and **2** were 10.32 and 10.18 min, respectively). Consistent with our expectations, [^{18}F]**2** exhibited a faster clearance from the brain than [^{18}F]**1**. In addition, the initial brain uptake of [^{18}F]**2** was higher than that of [^{11}C]SA4503 (3.61 ± 0.39% ID/g at 5 min),[34] [^{18}F]fluspidine (3.88 ± 0.92% ID/g at 5 min),[23] and [^{18}F]FP-fluspidine (3.66 ± 0.43% ID/g at 5 min).[27] Second, the radiotracer levels in the blood were relatively low with 1.62 ± 0.18% ID/g at 15 min and 1.38 ± 0.18% ID/g at 30 min p.i., resulting in high brain-to-blood ratios of 5.28 and 4.79 at 15 and 30 min, respectively. However, the brain-to-blood ratios of [^{18}F]**2** were lower than those of [^{18}F]**1**. Similar to the kinetic profile in the brain, [^{18}F]**2** also showed relatively fast washout in the organs known to contain σ_1 receptors, including the lungs, kidneys, heart, spleen, and liver. Finally, the accumulation of radiotracer in the bone increased slightly with time with 7.45% ID/g at 120 min, which was a little higher than that of [^{18}F]**1** with 6.13% ID/g, indicating that [^{18}F]**2** may undergo minimal defluorination in vivo.

In order to verify the specific binding of [^{18}F]**2** to σ_1 receptors in vivo, the effects of preadministration of haloperidol (0.1 mL, 1 mg/kg), compound **1** (0.1 mL, 1 mg/kg) and different concentrations of SA4503 (3, 5, or 10 μmol/kg) on the biodistribution of radiotracer in various organs of male ICR mice were investigated. Either saline or the blocking agents was injected 5 min prior to the radiotracer injection (0.1 mL, about 370 kBq). Blocking results of organ distribution of [^{18}F]**2** at 30 and 60 min postinjection in ICR mice are summarized in Figure 4. Pretreatment of animals with haloperidol, compound **1** and different concentrations of SA4503 resulted in significant reduction of radiotracer uptake in organs known to contain σ_1 receptors at 30 min, including the brain (72–74%, $p < 0.001$), heart (22–32%, $p < 0.05$), liver (32–50%, $p < 0.05$), spleen (47–70%, $p < 0.05$) and lungs (48–59%, $p < 0.05$ except for compound **1**). The corresponding blocking rate at 60 min was less than that at 30 min, including the brain (64–67%, $p < 0.001$), spleen (49–58%, $p < 0.05$) and lungs (34–43%, $p < 0.05$). These data demonstrated that [^{18}F]**2** binds to σ_1 receptors specifically in vivo.

2.3.3. Ex vivo autoradiography in Sprague–Dawley rats

To evaluate the potential use of [^{18}F]**2** for σ_1 receptor imaging in the brain, an ex vivo autoradiography at 1 h after injection of [^{18}F]**2** (0.3 mL, 74.0 MBq) was performed to investigate the distribution of [^{18}F]**2** in different brain regions in Sprague–Dawley rats. The results are presented in Figure 5. Similar to what was found for [^{18}F]**1**,[29] high accumulation of radiotracer was observed in the cortex, particularly in the temporal cortex auditory area. In the cerebellum, comparably high uptake was found in the vermian lobule and low uptake in the paramedian lobule. In the brain areas known to possess high expression of σ_1 receptors, such as thalamus, hypothalamus, midbrain, red nucleus, and facial nucleus, high accumulation of the radiotracer was also observed, which is consistent with the brain distribution of [^{11}C]SA4503.[35] In addition, high accumulation was observed in the medulla oblongata. Moderate accumulation of radiotracer was observed in the hippocampus and striatum. Comparably low accumulation was observed in the nucleus accumbens and olfactory bulb. Taken together, the accumulation of the radiotracer in the rat brain is in good agreement with the density profile of σ_1 receptors.

Table 2
Biodistribution of [^{18}F]**2** in male ICR mice[a]

Organ	2 min	15 min	30 min	60 min	120 min
Blood	2.59 ± 0.28	1.62 ± 0.18	1.38 ± 0.18	1.43 ± 0.19	1.90 ± 0.08
Brain	8.39 ± 1.54	8.56 ± 0.34	6.61 ± 1.22	4.62 ± 0.17	3.31 ± 0.33
Heart	13.29 ± 2.49	6.66 ± 1.06	3.49 ± 0.52	3.08 ± 0.86	2.83 ± 0.78
Liver	6.97 ± 1.15	6.72 ± 1.29	6.95 ± 1.35	5.42 ± 0.89	3.74 ± 0.37
Spleen	4.10 ± 0.56	8.67 ± 1.51	6.76 ± 1.11	5.95 ± 0.81	4.13 ± 0.37
Lung	38.45 ± 8.14	10.26 ± 1.41	6.23 ± 1.89	4.34 ± 0.30	2.65 ± 0.30
Kidney	23.60 ± 1.23	13.00 ± 1.94	7.83 ± 1.14	6.97 ± 2.36	3.79 ± 0.28
Small intestine [b]	5.07 ± 1.33	6.43 ± 0.60	4.73 ± 1.86	5.74 ± 1.67	6.34 ± 1.61
Stomach [b]	1.41 ± 0.27	1.84 ± 0.44	1.23 ± 0.49	1.08 ± 0.23	0.89 ± 0.14
Muscle	2.78 ± 0.14	2.62 ± 0.48	1.98 ± 0.24	2.10 ± 0.30	1.61 ± 0.29
Bone	2.64 ± 0.72	3.70 ± 0.66	5.61 ± 0.89	6.28 ± 1.47	7.45 ± 0.75
Brain/blood	3.24	5.28	4.79	3.23	1.74

[a] Data are means of % ID/g of tissue ± SD, n = 5.
[b] % ID/organ.

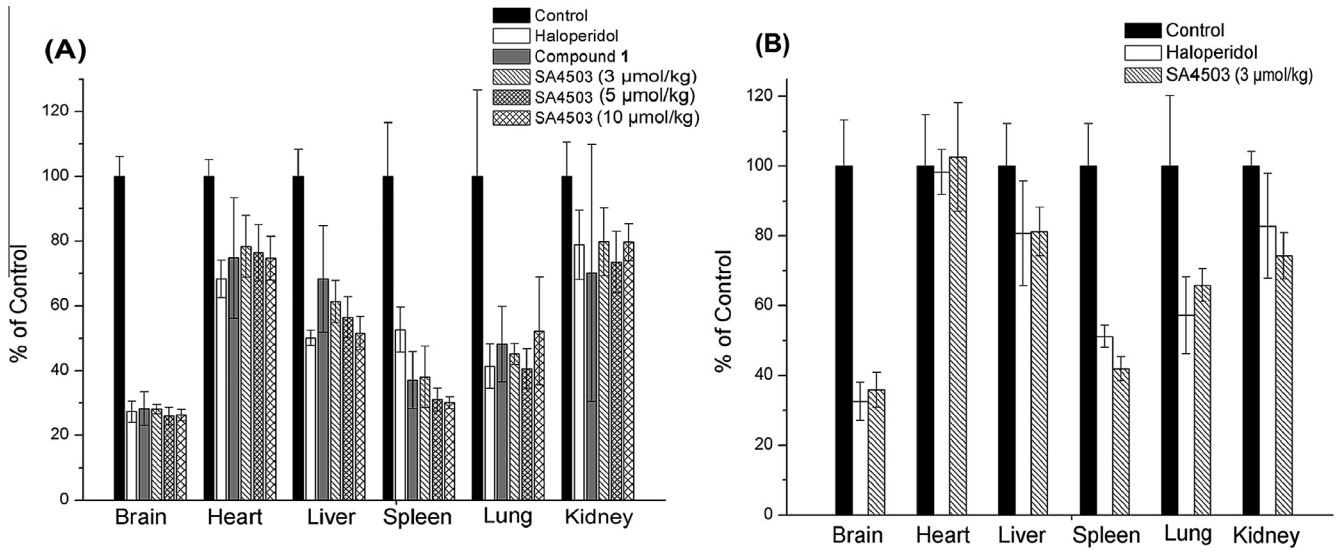

Figure 4. (A) Effects of preadministration of haloperidol (0.1 mL, 1 mg/kg), compound **1** (0.1 mL, 1 mg/kg) and different concentrations of SA4503 (3, 5, or 10 μmol/kg) on organ distribution of [^{18}F]**2** (0.1 mL, about 370 kBq) 30 min after intravenous injection. Student's *t* test (independent, two-tailed) was performed, and $p < 0.05$ (except for compound **1** in the lungs and in the kidney, SA4503 (3 μmol/kg) in the kidney). (B) Effects of preadministration of haloperidol (0.1 mL, 1 mg/kg) and SA4503 (0.1 mL, 3 μmol/kg) 5 min prior to the injection of radiotracer [^{18}F]**2** (0.1 mL, about 370 kBq) 60 min after intravenous administration. Student's *t* test (independent, two-tailed) was performed, and $p < 0.05$ (except for haloperidol and SA4503 in the heart, haloperidol in the liver). Values are means ± SD, $n = 5$.

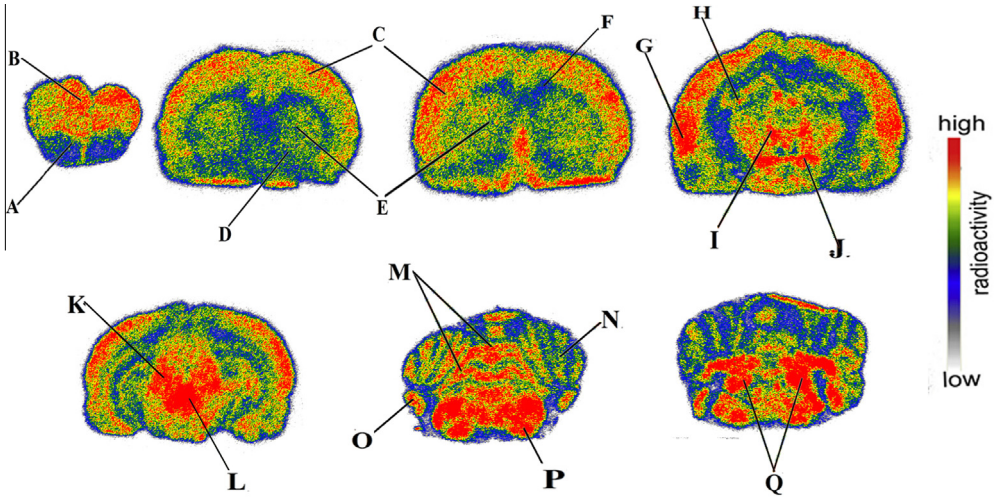

Figure 5. Ex vivo autoradiograms of the rat coronal brain slices at 60 min after intravenous injection of [^{18}F]**2** (0.3 mL, 74.0 MBq). (A) Olfactory bulb; (B) Frontal cortex; (C) Cerebral cortex; (D) Nucleus accumbens; (E) Striatum; (F) Cingulate cortex (G) Temporal cortex auditory; (H) Hippocampus; (I) Thalamus; (J) Hypothalamus; (K) Midbrain; (L) Red nucleus; (M) Vermian lobule; (N) Paramedian lobule (O) Paraflocculus; (P) Facial nucleus; (Q) Medulla Oblongata.

2.3.4. In vivo metabolism of [^{18}F]2

For development of a radiotracer for brain imaging, it is necessary to investigate the metabolism profile of the radiotracer in vivo. Therefore, the metabolic profile of [^{18}F]**2** was investigated in plasma, liver and brain samples obtained from mice at 30 and 60 min p.i., respectively. Protein precipitation was performed by using ice-cold acetonitrile. Acetonitrile extracts were analyzed and quantified by radio-HPLC. Representative HPLC chromatograms are given in Figure 6. Additional HPLC chromatograms are presented in Table S1 (Supplementary data).

At 30 min p.i., about 77% of the total radioactivity was represented by [^{18}F]**2** (retention time of 10.76 min) in plasma samples. Two hydrophilic radioactive metabolites M1 (19%) and M2 (4%) were observed with retention times of 2.18 and 2.92 min, respectively. In liver homogenates, 49% of total radioactivity accounted for [^{18}F]**2** at 30 min p.i., while 8%, 2%, 13% and 29% accounted for metabolites M1, M2, M3 and M4 with retention times of 2.18, 2.93, 4.86 and 7.81 min, respectively. Similar to what were found for [^{18}F]fluspidine,[23] there were two radiometabolites (M3 and M4) not detected in plasma samples. In the brain samples, about 93% of the total radioactivity was represented by the parent radiotracer [^{18}F]**2**.

At 60 min p.i., the percentage of parent tracer was decreased rapidly to 3% in plasma samples. The percentage of the major metabolite M1 increased to 87% (Fig. S4, Supplementary data). Only 38% of the parent radiotracer remained in the brain. Identities of the radioactive metabolites of [^{18}F]**2** formed in the periphery needs to be investigated further.

Recently, more and more evidence suggests that σ_1 receptors are linked to many human brain diseases.[5–8] Neuroimaging of σ_1 receptors with PET radiotracers provides an important tool to investigate the involvement of σ_1 receptors in the pathophysiology of neuropsychiatric diseases.[14] However, among the potential PET radiotracers, use of [^{11}C]SA4503 needs an on-site cyclotron.

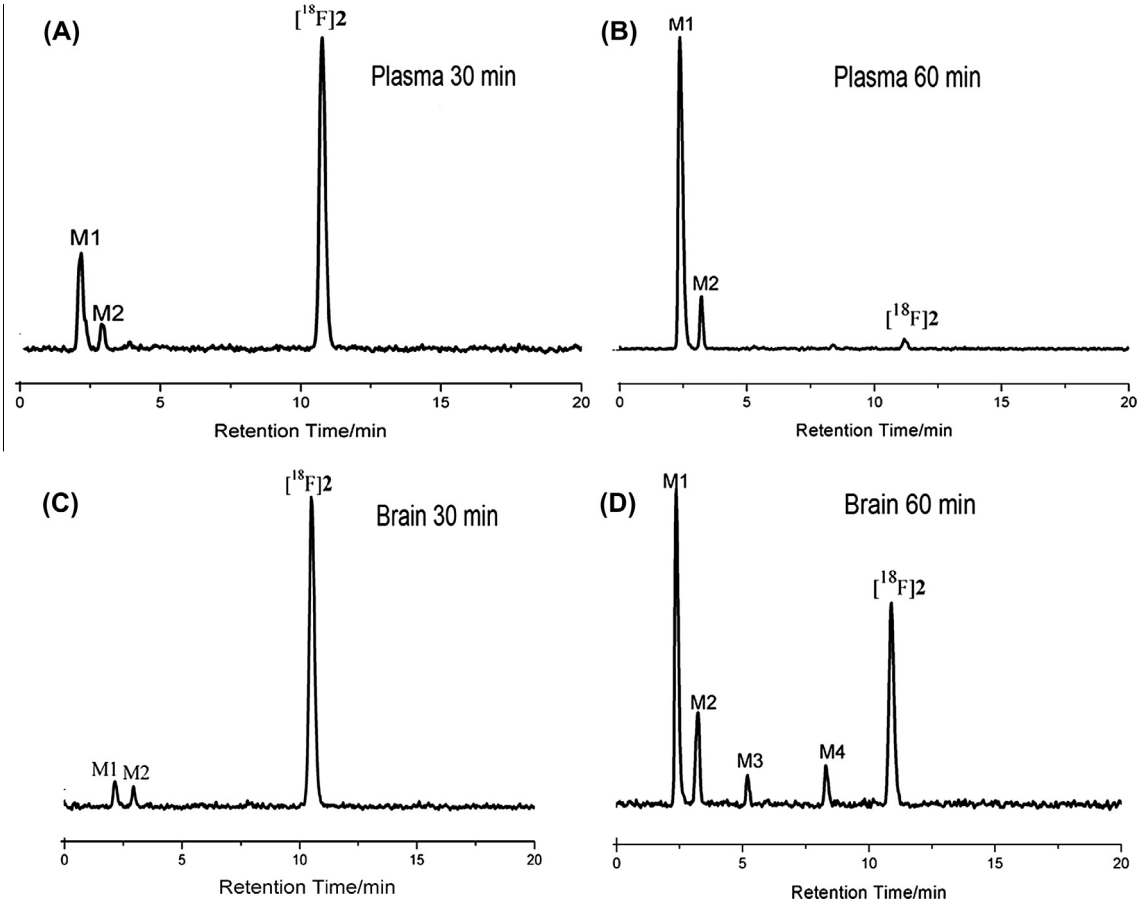

Figure 6. Analytical radio-HPLC chromatograms of the plasma and brain extracts at 30 and 60 min after administration of [^{18}F]**2** in mice.

[^{18}F]FPS[20] was found to have irreversible kinetics in humans. Prospects of [^{18}F]fluspidine[23] and [^{18}F]FTC-146[24,25] for eventual clinical translation require further investigation. In our previous work,[29] we have found that [^{18}F]**1** is a promising σ_1 receptor imaging agent with subnanomolar affinity for σ_1 receptors, excellent σ_1/σ_2 subtype selectivity, and high σ_1/VAChT selectivity. Moreover, no binding to EBP, dopamine D_2/D_3 receptors and 5-HTT of [^{18}F]**1** was observed. However, [^{18}F]**1** was found to clear rather slowly from the brain. In order to find suitable ^{18}F-labeled radiotracers, especially to avoid irreversible binding kinetics, we designed and synthesized some fluoroalkoxy analogues. Among them, compound **2** possesses nanomolar affinity for σ_1 receptors and high selectivity over σ_2 receptors and VAChT as well as the lowest lipophilicity. So [^{18}F]**2** was synthesized and evaluated for its potential as σ_1 receptor radiotracer. High in vitro stability of [^{18}F]**2** in mouse plasma was observed. In addition, replacement of the benzene ring with pyridine slightly decreases the lipophilicity of the compound. In the biodistribution studies, the initial brain uptake of [^{18}F]**2** was observed to be a little lower than that of [^{18}F]**1**. But it was still higher than that of [^{11}C]SA4503,[34] [^{18}F]fluspidine,[23] and [^{18}F]FP-fluspidine.[27] More importantly, [^{18}F]**2** exhibited a faster clearance from the brain and other organs known to contain σ_1 receptors, which was in good agreement with the lower affinity of [^{18}F]**2**. Currently, haloperidol is recognized as the most widely used σ_1 antagonist in research on σ_1 receptors. Based on the results reported in the literature, SA4503 possesses high affinity for σ_1 receptors and low to negligible affinity for 36 other receptors, ion channels and second messenger systems.[36] So SA4503 has also been used as blocking agent to determine target specificity.[37] In addition, compound **1** proved to possess excellent affinity and selectivity for σ_1 receptors. So we used haloperidol, compound **1** and SA4503 as blocking agents for assessing the binding specificity of [^{18}F]**2** to σ_1 receptors in vivo. It is encouraging that the percentage of specific uptake of [^{18}F]**2** in the brain was higher than that of [^{18}F]**1** (67% vs 58% for [^{18}F]**2** and [^{18}F]**1** at 60 min p.i.), which is consistent with our expectations that lower lipophilicity could decrease the non-specific binding in vivo. To evaluate the potential use of [^{18}F]**2** for imaging σ_1 receptor density in the brain, we performed ex vivo autoradiography study to investigate the accumulation of [^{18}F]**2** in different brain regions in Sprague–Dawley rats. High accumulation of radiotracer was observed in brain areas known to have high expression of σ_1 receptors.

It is well known that investigation of a radioligand's metabolism profile in vivo is also very important. Therefore, in vivo metabolic fate of [^{18}F]**2** in the plasma, brain and liver of male ICR mice at 30 and 60 min was investigated. Results showed that the parent compound [^{18}F]**2** and two likely polar radioactive metabolites were found in the mouse plasma. As indicated in the literature for the plasma metabolic profile of [^{18}F]AV-45,[38] in addition to the parent radiotracer, three metabolite peaks were observed in plasma. However, it seemed unlikely that plasma levels of radioactive metabolites could be high enough to account for the observed tracer activity in the brain. In this study, only two likely polar metabolites were observed both at 30 and 60 min after injection of [^{18}F]**2**. Thus, if radioactive metabolites of [^{18}F]**2** may make some contribution, particularly to the nontarget activity, they have minimal influence on the specific binding signal of [^{18}F]**2** to σ_1 receptors in the brain. In the brain, the percentage of [^{18}F]**2** at 30 min p.i. was higher than that at 60 min (93% vs 38%), which was in accord with higher percentage of specific binding of [^{18}F]**2** at 30 min.

Currently, the identities of the radioactive metabolites have not been determined. Moreover, selectivity over other neuroreceptors

of [^{18}F]**2** should be taken into consideration. These further investigations and small animal PET imaging studies are in progress to evaluate [^{18}F]**2** as a candidate for σ_1 receptor imaging with PET in humans.

3. Conclusion

We have successfully synthesized [^{18}F]**2** as a novel radiotracer for σ_1 receptor imaging using an efficient one-pot, two-step reaction sequence in a home-made automated synthesis module. In biodistribution studies in mice [^{18}F]**2** displayed high initial brain uptake and relatively fast clearance from the brain. Blocking studies confirmed high specific binding of [^{18}F]**2** to σ_1 receptors in vivo. Ex vivo autoradiography indicated that accumulation of the radiotracer in the rat brain was in good agreement with the density profile of σ_1 receptors. In vivo metabolic studies suggested that radioactive metabolites of [^{18}F]**2** have minimal influence on the specific binding signal to σ_1 receptors in the brain. These findings warrant further evaluation of the potential of [^{18}F]**2** as a radiotracer for investigation of σ_1 receptors with PET in humans.

4. Experimental section

4.1. General method

All reagents and solvents were obtained in high purity from commercial sources and used without further purification unless otherwise stated. Reactions were monitored by thin-layer chromatography (TLC) (TLC silica gel 60 F_{254} plates Merck). Flash column chromatography was carried out on silica gel (200–400 mesh) using the solvent system indicated in the experimental procedure. HPLC methods were used to determine the purity of the test compounds used in the binding assays. ^{1}H NMR spectra were recorded on a Bruker Avance III (400 MHz) NMR spectrometer. Chemical shift (δ) are reported in ppm downfield from tetramethylsilane and coupling constants (J) in Hertz (Hz). ^{13}C NMR spectra were recorded on a Bruker Avance III (100 MHz) NMR spectrometer. MS spectra were obtained by microTOF-QII ESI/MS (Bruker, USA).

HPLC separations were performed in the PET-MF-2V-IT-1 multifunctional synthesis module. The semi-preparative radio-HPLC was equipped with an Alltech 626 pump and UVSI 200 detector. Samples were separated on an Agela Venusil MP C18 column (250 mm × 10 mm, 5 μm) using acetonitrile and water (containing 10 mM NH_4OAc) (40:60, v/v) as mobile phase at a flow rate of 4 mL/min.

HPLC analyses for the identification of the radiotracer and for the investigation of in vitro stability and in vivo metabolism of [^{18}F]**2** were performed on a Waters 600 system (Waters, corporation, USA) equipped with a Waters 2489 UV–VIS detector and a Raytest Gabi NaI (Tl) scintillation detector (Raytest, Germany). Samples were analyzed on an Agela Venusil MP C18 column (250 mm × 4.6 mm, 5 μm) using acetonitrile and water (containing 10 mM NH_4OAc) (60:40, v/v) as mobile phase at a flow rate of 1 mL/min.

Male ICR mice (4–5 weeks, 22–25 g) and Sprague–Dawley rats (male, 9 weeks old, 220–250 g) were purchased from Peking University Health Science Center. All procedures of the animal experiments were performed in compliance with relevant laws and institutional guidelines. All of the animal experiments were approved by the Institutional Animal Care and Use Committee of Beijing Normal University.

4.2. 1′-(4-(3-Fluoropropoxy)benzyl)-3*H*-spiro[2-benzofuran-1,4′-piperidine] (3)

Compound **9** (45.0 mg, 0.15 mmol) was dissolved in anhydrous CH_3CN (10 mL), followed by addition of **7** (35.0 mg, 0.15 mmol) and K_2CO_3 (41.0 mg, 0.30 mmol). The mixture was heated to reflux for 18 h. The mixture was concentrated under vacuum and the residue was dissolved in CH_2Cl_2, washed with water, dried with $MgSO_4$ and concentrated under vacuum. The crude product was purified by silica gel chromatography (ethyl acetate/petroleum ether = 1/1, v/v) to provide **3** as colorless oil (33.0 mg, 61%). ^{1}H NMR (400 MHz, $CDCl_3$) δ (ppm): 7.28–7.26 (m, 4H), 7.21–7.16 (m, 2H), 6.89 (s, 1H), 6.87 (s, 1H), 5.07 (s, 2H), 4.71 (t, J = 5.8 Hz, 1H), 4.60 (t, J = 5.8 Hz, 1H), 4.10 (t, J = 6.1 Hz, 2H), 3.57 (s, 2H), 2.86 (s, 2H), 2.42 (s, 2H), 2.24–2.11 (m, 2H), 2.02 (s, 2H), 1.79 (s, 1H), 1.75 (s, 1H). ^{13}C NMR (100 MHz, $CDCl_3$) δ 157.98, 145.77, 138.98, 130.65, 130.44, 127.59, 127.38, 121.08, 120.89, 114.24, 84.80, 81.64, 80.00, 77.30, 70.77, 63.53, 63.48, 62.83, 50.05, 36.61, 30.60, 30.40. ESI-TOF MS calcd for $C_{22}H_{27}FNO_2$ $[M+H]^+$: 356.2068; found: 356.2087.

4.3. 1′-((6-(3-Fluoropropoxy)pyridin-3-yl)methyl)-3*H*-spiro[2-benzofuran-1,4′-piperidine] (4)

The procedure described for the synthesis of **3** was applied to **10** to provide **4** as colorless oil (12.0 mg, 33%). ^{1}H NMR (400 MHz, $CDCl_3$) δ (ppm): 8.08 (s, 1H), 7.74 (s, 1H), 7.29–7.21 (m, 4H), 6.76–6.74 (d, J = 8.1 Hz, 1H), 5.07 (s, 2H), 4.70 (t, J = 5.8 Hz, 1H), 4.58 (t, J = 5.8 Hz, 1H), 4.43 (t, J = 6.2 Hz, 2H), 3.62 (s, 2H), 2.92 (s, 2H), 2.54 (s, 2H), 2.22–2.05 (m, 4H), 1.80 (s, 1H), 1.77 (s, 1H). ESI-TOF MS calcd for $C_{21}H_{26}FN_2O_2$ $[M+H]^+$: 357.1973; found: 357.1996.

4.4. (4-((3*H*-Spiro[2-benzofuran-1,4′-piperidin]-1′-yl)methyl) phenyl)methanol (11)

Compound **8** (50.0 mg, 0.26 mmol) was dissolved in 1,2-dichloroethane (10 mL), followed by addition of 4-(hydroxymethyl)benzaldehyde (40.0 mg, 0.29 mmol). The mixture was stirred at room temperature for 2 h, followed by addition of $NaBH(OAc)_3$ (63.0 mg, 0.30 mmol). The mixture was stirred for an additional 48 h. Then the reaction was quenched with saturated $NaHCO_3$, evaporated to remove the organic solvent, and extracted with ethyl acetate. The combined organic layers were dried with $MgSO_4$, and concentrated under vacuum. The residue was purified by silica gel chromatography (ethyl acetate/petroleum ether = 2/1, v/v) to provide **11** as colorless oil (27.0 mg, 33%). ^{1}H NMR (400 MHz, $CDCl_3$) δ (ppm): 7.26 (s, 3H), 7.20–7.19 (m, 3H), 7.18–7.16 (m, 2H), 6.79 (br s, 1H), 5.04 (s, 2H), 3.79 (s, 2H), 3.08 (s, 1H), 3.05 (s, 1H), 2.65 (td, J = 4.32, 13.68 Hz, 2H), 2.06 (s, 2H), 1.76 (s, 1H), 1.73 (s, 1H). ESI-MS, $[M+H]^+$: m/z = 311.0.

4.5. 1′-(4-((2-Fluoroethoxy)methyl)benzyl)-3*H*-spiro[2-benzofuran-1,4′-piperidine] (5)

A mixture of **11** (27.0 mg, 0.09 mmol), 1-bromo-2-fluoroethane (218.0 mg, 1.72 mmol) and K_2CO_3 (194.0 mg, 1.40 mmol) in acetone (30 mL) was heated at 60 °C for 10 h, followed by addition of saturated NH_4Cl to neutralize the mixture. The aqueous phase was extracted with ethyl acetate. The combined organic phases were dried over $MgSO_4$ and concentrated under vacuum. The crude product was purified by silica gel column chromatography (ethyl acetate/petroleum ether = 1/4, v/v) to provide **5** as a white solid (10.0 mg, 32%). ^{1}H NMR (400 MHz, $CDCl_3$) δ (ppm): 7.37–7.31 (m, 4H), 7.27–7.26 (m, 2H), 7.21–7.19 (m, 1H), 7.16–7.14 (m, 1H), 5.07 (s, 2H), 4.65 (t, J = 4.1 Hz, 1H), 4.59 (s, 2H), 4.54 (t, J = 4.1 Hz, 1H), 3.77 (t, J = 4.1 Hz, 1H), 3.69 (t, J = 4.1 Hz, 1H), 3.60 (s, 2H), 2.87 (s, 1H), 2.84 (s, 1H), 2.44 (t, J = 11.6 Hz, 2H), 2.21 (t, J = 12.0 Hz, 2H), 1.77 (s, 1H), 1.74 (s, 1H). ^{13}C NMR (100 MHz, $CDCl_3$) δ 145.71, 138.96, 136.66, 129.52, 127.81, 127.59, 127.37, 121.07, 120.87, 84.72, 84.02, 82.34, 77.27, 73.26, 70.26, 69.33,

69.13, 63.12, 50.14, 36.58, 30.96. ESI-TOF MS calcd for $C_{22}H_{27}FNO_2$ $[M+H]^+$: 356.2020; found: 356.2074.

4.6. Radiochemistry

The synthesis of radiotracer [^{18}F]**2** was performed in a homemade synthesis module. [^{18}F]fluoride was produced through the nuclear reaction of $^{18}O(p, n)^{18}F$ using proton beam bombardment of the target (20 MeV, 65 μA) for 15 min in a Sumitomo HM-20S cyclotron. Then [^{18}F]fluoride was transported to the QMA column of the multifunctional synthesis module (PET-MF-2V-IT-I) via nitrogen carrier gas, and eluted into a reaction vessel using a solution of Kryptofix 2.2.2 (13 mg) and potassium carbonate (1.1 mg) in CH_3CN/H_2O (0.8 mL/0.2 mL). The solvent was removed at 115 °C under a stream of nitrogen. The residue was azeotropically dried three times with 1 mL of anhydrous acetonitrile each at 115 °C, followed by adding a solution of the tosylate precursor **12** (8 mg/mL) in anhydrous acetonitrile (1 mL). The mixture was stirred at 90 °C for 15 min to provide compound **13**. After the solvent was removed under a stream of nitrogen, a solution of compound **10** (7 mg) and NaOH (20 μL, 2 mol/L) in DMSO (0.5 mL) was added to the reaction vessel. The mixture was heated at 110 °C for 20 min, followed by addition of the HPLC eluent (2 mL) to quench the reaction, and loaded onto a sample loop in the isocratic semi-preparative radio-HPLC for purification (Agela Venusil MP C18 column, 250 mm × 10 mm, 5 μm, eluent 40% CH_3CN and 60% H_2O containing 10 mM NH_4OAc, flow rate 4 mL/min). The product peak was collected, diluted with water and trapped on a Waters C18 plus Sep-Pak cartridge. The product was eluted off the cartridge with ethanol. Radiochemical purity was analyzed by analytical radio-HPLC (Agela Venusil MP C18 column, 250 mm × 4.6 mm, 5 μm, eluent 60% CH_3CN and 40% H_2O containing 10 mM NH_4OAc, flow rate 1 mL/min). Specific activity was determined with a HPLC-based method. For animal experiments, [^{18}F]**2** was formulated as a saline solution containing no more than 8% ethanol.

4.7. Determination of log*D* value

The apparent distribution coefficient of [^{18}F]**2** was determined by measuring the distribution of the radiotracer between 1-octanol and potassium phosphate buffer (PBS, 0.05 mol/L, pH 7.4). The radiotracer [^{18}F]**2** (10 μL, 540 kBq) was mixed with 1-octanol (3 mL) and potassium phosphate buffer (3 mL) in a centrifuge tube (15 mL). The tube was vortexed for 3 min, followed by centrifugation at 3500 rpm for 5 min (AnkeTDL80-2B, China). About 0.05 mL of 1-octanol layer was weighed in a tared tube. About 0.5 mL of the PBS layer was weighed in a second tared tube. After addition of 0.5 mL of buffer to the 1-octanol fraction and 0.05 mL of 1-octanol to the aqueous fraction, activity in both tubes was measured in an automatic γ-counter (Wallac 1470 Wizard, United States). The log*D* value was calculated as the ratio of the cpm/mL of 1-octanol to that of PBS and expressed as $\log D = \log[\text{cpm/mL}(1-\text{octanol})/\text{cpm/mL}(\text{PBS})]$. Samples from the remaining organic layer were repartitioned until consistent distribution coefficient values were obtained. The measurement was carried out in triplicate and repeated three times.

4.8. In vitro stability studies

The in vitro stability of [^{18}F]**2** was evaluated by monitoring the radiochemical purity at different time points. To 0.3 mL of freshly prepared mouse plasma, 0.2 mL of [^{18}F]**2** solution was added and incubated at 37 °C in an Electric Thermostatic Incubator (DH-250). At 2 and 4 h, the mixture was treated with 0.4 mL of ice-cold CH_3CN, and vortexed for 1 min. The plasma samples were centrifuged at 14000 rpm for 5 min. The supernatants of each sample were passed through an organic Millipore filter (0.22 μm) and analyzed by radio-HPLC (Water 600 system, Agela Venusil MP C18 column, 250 mm × 4.6 mm, 5 μm, eluent 60% CH_3CN and 40% H_2O containing 10 mM NH_4OAc, flow rate 1 mL/min).

4.9. In vitro binding assays

All the procedures for the σ receptor competition studies were previously described. Briefly, the σ_1 receptor assay was carried out with (+)-[^{3}H]-pentazocine as the radioligand using rat brain membrane homogenates. The σ_2 receptor affinity was performed using rat liver membrane homogenates with the radioligand [^{3}H]DTG in the presence of 10 μM dextrallorphan for selective masking of σ_1 receptor binding sites. Nonspecific binding was determined with addition of 10 μM haloperidol. K_i values were calculated according to the Cheng-Prusoff equation and represent data from at least two independent experiments, each performed in triplicate. The results are given as mean ± standard deviation (SD).

4.10. Biodistribution and blocking studies in male ICR mice

A saline solution of [^{18}F]**2** (0.1 mL, about 370 kBq) was intravenously injected into mice (five groups, $n = 5$ in each group) via the tail vein. The mice were sacrificed by decapitation at 2, 15, 30, 60 and 120 min p.i. Samples of blood, whole brain, heart, liver, spleen, lungs, kidneys, muscle and bone were removed, weighed and counted in an automatic γ-counter (Wallac 1470 Wizard, USA). The percentage of injected dose per gram of wet tissue (% ID/g) was calculated by a comparison of the tissue count to suitably diluted aliquots of the injected radiotracer as counting standards. All radioactivity measurements were corrected for decay. The results are given as mean ± standard deviation (SD).

For the blocking studies, the mice were injected via the tail vein with either saline (0.1 mL) or a blocking agent, including haloperidol (0.1 mL, 1 mg/kg), compound **1** (0.1 mL, 1 mg/kg), SA4503 (0.1 mL, 3 μmol/kg), SA4503 (0.1 mL, 5 μmol/kg) or SA4503 (0.1 mL, 10 μmol/kg) 5 min prior to the injection of [^{18}F]**2** (0.1 mL, about 370 kBq). The mice were sacrificed by decapitation at 30 or 60 min after radiotracer injection. The blood and organs of interest were isolated and analyzed as described above. Significant differences between control and test groups were determined by Student's *t* test (independent, two-tailed). The criterion for significance was $p \leqslant 0.05$. Data given in the figures are mean values ± standard deviation (SD).

4.11. Ex vivo autoradiography of [^{18}F]2 in rat brain

Ex vivo autoradiography was carried out in male Sprague–Dawley rats (9 weeks, 220–250 g). A solution of [^{18}F]**2** (0.3 mL, 74.0 MBq) was intravenously injected into conscious rats via the tail vein. The rats were killed by cervical dislocation at 60 min after administration of the radioligand. The brain was rapidly removed, frozen at −80 °C in a liquid nitrogen bath. The coronal brain sections (20 μm) were consecutively cut on a cryotome (CM1900, Leica, Germany). The brain slices were dried at room temperature and exposed to a phosphor plate film (PerkinElmer, USA) for 2 h. Autoradiographic images were obtained using a phosphor imaging system (Cyclone Plus, PerkinElmer, USA) and analyzed with the AIDA 2.31 software (Raytest, Straubenhardt, Germany).

4.12. In vivo metabolism of [^{18}F]2

The in vivo metabolism of [^{18}F]**2** was performed in male ICR mice. The mice were intravenously injected with a saline solution of [^{18}F]**2** (0.1 mL, 18.5 MBq) via the tail vein and sacrificed by decapitation at 30 or 60 min postinjection, respectively. The

plasma, brain and liver were collected. The brain and liver were washed with saline. The samples were placed separately in 2 mL of ice-cold saline and homogenized with a homogenizer (LabGEN 7) for 2 min. Ice-cold CH_3CN (10 mL) was added to the homogenates. The mixtures were vortexed for 1 min and centrifuged at 14000 rpm for 5 min (Eppendorf Centrifuge 5418). The combined supernatants were collected and passed through a 0.22 μm organic Millipore filter. The filtrates were concentrated to 0.1 mL under a stream of nitrogen gas flow and injected into the radio-HPLC for analysis (Water 600 system, Agela Venusil MP C18 column, 250 mm × 4.6 mm, 5 μm, eluent 60% CH_3CN and 40% H_2O containing 10 mM NH_4OAc, flow rate 1 mL/min).

Acknowledgment

This work was supported by the national Natural Science Foundation of China (No. 21071023).

Supplementary data

Supplementary data associated with this article can be found, in the online version, at http://dx.doi.org/10.1016/j.bmc.2014.08.003.

References and notes

1. Hanner, M.; Moebius, F. F.; Flandorfer, A.; Knaus, H. G.; Striessnig, J.; Kempner, E.; Glossmann, H. *Proc. Natl. Acad. Sci. U.S.A.* **1996**, *93*, 8072.
2. Aydar, E.; Palmer, C. P.; Klyachko, V. A.; Jackson, M. B. *Neuron* **2002**, *34*, 399.
3. Hayashi, T.; Su, T.-P. *Cell* **2007**, *131*, 596.
4. Su, T.-P.; Hayashi, T.; Maurice, T.; Buch, S.; Ruoho, A. E. *Trends Pharmacol. Sci.* **2010**, *31*, 557.
5. Maurice, T.; Su, T.-P. *Pharmacol. Ther.* **2009**, *124*, 195.
6. Hayashi, T.; Tsai, S.-Y.; Mori, T.; Fujimoto, M.; Su, T.-P. *Expert Opin. Ther. Targets* **2011**, *15*, 557.
7. Kourrich, S.; Su, T.-P.; Fujimoto, M.; Bonci, A. *Trends Neurosci.* **2012**, *35*, 762.
8. Bourrie, B.; Bribes, E.; Derocq, J.-M.; Vidal, H.; Casellas, P. *Curr. Opin. Invest. Drugs* **2004**, *5*, 1158.
9. Ito, K.; Hirooka, Y.; Matsukawa, R.; Nakano, M.; Sunagawa, K. *Cardiovasc. Res.* **2012**, *93*, 33.
10. Hashimoto, K. *Prog. Neurobiol.* **2013**, *100*, 15.
11. van Waarde, A.; Rybczynska, A. A.; Ramakrishnan, N. K.; Ishiwata, K.; Elsinga, P. H.; Dierckx, R. A. J. O. *Curr. Pharm. Des.* **2010**, *16*, 3519.
12. Megalizzi, V.; Le Mercier, M.; Decaestecker, C. *Med. Res. Rev.* **2012**, *32*, 410.
13. Simony-Lafontaine, J.; Esslimani, M.; Bribes, E.; Gourgou, S.; Lequeux, N.; Lavail, R.; Grenier, J.; Kramar, A.; Casellas, P. *Br. J. Cancer* **2000**, *82*, 1958.
14. Brust, P.; Deuther-Conrad, W.; Lehmkuhl, K.; Jia, H.; Wunsch, B. *Curr. Med. Chem.* **2014**, *21*, 35.
15. Mishina, M.; Ohyama, M.; Ishii, K.; Kitamura, S.; Kimura, Y.; Oda, K.-I.; Kawamura, K.; Sasaki, T.; Kobayashi, S.; Katayama, Y.; Ishiwata, K. *Ann. Nucl. Med.* **2008**, *22*, 151.
16. Mishina, M.; Ishiwata, K.; Ishii, K.; Kitamura, S.; Kimura, Y.; Kawamura, K.; Oda, K.; Sasaki, T.; Sakayori, O.; Hamamoto, M.; Kobayashi, S.; Katayama, Y. *Acta Neurol. Scand.* **2005**, *112*, 103.
17. Toyohara, J.; Sakata, M.; Ishiwata, K. *Cent. Nerv. Syst. Agents Med. Chem.* **2009**, *9*, 190.
18. Waterhouse, R. N.; Nobler, M. S.; Zhou, Y.; Chang, R. C.; Morales, O.; Kuwabawa, H.; Kumar, A.; VanHeertum, R. L.; Wong, D. F.; Sackeim, H. A. *Neuroimage* **2004**, *22*, T29.
19. Stone, J. M.; Årstad, E.; Erlandsson, K.; Waterhouse, R. N.; Ell, P. J.; Pilowsky, L. S. *Synapse* **2006**, *60*, 109.
20. Waterhouse, R. N.; Chang, R. C.; Atuehene, N.; Collier, T. L. *Synapse* **2007**, *61*, 540.
21. Shiba, K.; Ogawa, K.; Ishiwata, K.; Yajima, K.; Mori, H. *Bioorg. Med. Chem.* **2006**, *14*, 2620.
22. Ishiwata, K.; Kawamura, K.; Yajima, K.; QingGeLeTu; Mori, H.; Shiba, K. *Nucl. Med. Biol.* **2006**, *33*, 543.
23. Fischer, S.; Wiese, C.; Große Maestrup, E.; Hiller, A.; Deuther-Conrad, W.; Scheunemann, M.; Schepmann, D.; Steinbach, J.; Wünsch, B.; Brust, P. *Eur. J. Nucl. Med. Mol.* **2011**, *38*, 540.
24. James, M. L.; Shen, B.; Zavaleta, C. L.; Nielsen, C. H.; Mesangeau, C.; Vuppala, P. K.; Chan, C.; Avery, B. A.; Fishback, J. A.; Matsumoto, R. R.; Gambhir, S. S.; McCurdy, C. R.; Chin, F. T. *J. Med. Chem.* **2012**, *55*, 8272.
25. James, M. L.; Shen, B.; Nielsen, C. H.; Behera, D.; Buckmaster, C. L.; Mesangeau, C.; Zavaleta, C.; Vuppala, P. K.; Jamalapuram, S.; Avery, B. A.; Lyons, D. M.; McCurdy, C. R.; Biswal, S.; Gambhir, S. S.; Chin, F. T. *J. Nucl. Med.* **2014**, *55*, 147.
26. Große Maestrup, E.; Wiese, C.; Schepmann, D.; Hiller, A.; Fischer, S.; Scheunemann, M.; Brust, P.; Wünsch, B. *Bioorg. Med. Chem.* **2009**, *17*, 3630.
27. Große Maestrup, E.; Fischer, S.; Wiese, C.; Schepmann, D.; Hiller, A.; Deuther-Conrad, W.; Steinbach, J. R.; Wünsch, B.; Brust, P. *J. Med. Chem.* **2009**, *52*, 6062.
28. Maisonial, A.; Große Maestrup, E.; Wiese, C.; Hiller, A.; Schepmann, D.; Fischer, S.; Deuther-Conrad, W.; Steinbach, J.; Brust, P.; Wünsch, B. *Bioorg. Med. Chem.* **2012**, *20*, 257.
29. Li, Y.; Wang, X.; Zhang, J.; Deuther-Conrad, W.; Xie, F.; Zhang, X.; Liu, J.; Qiao, J.; Cui, M.; Steinbach, J.; Brust, P.; Liu, B.; Jia, H. *J. Med. Chem.* **2013**, *56*, 3478.
30. Moussa, I. A.; Banister, S. D.; Beinat, C.; Giboureau, N.; Reynolds, A. J.; Kassiou, M. *J. Med. Chem.* **2010**, *53*, 6228.
31. Kubota, H.; Fujii, M.; Ikeda, K.; Takeuchi, M.; Shibanuma, T.; Isomura, Y. *Chem. Pharm. Bull.* **1998**, *46*, 351.
32. Fan, C.; Jia, H.; Deuther-Conrad, W.; Brust, P.; Steinbach, J.; Liu, B. *Sci. China Ser. B* **2006**, *49*, 169.
33. Sorger, D.; Scheunemann, M.; Grossmann, U.; Fischer, S.; Vercouille, J.; Hiller, A.; Wenzel, B.; Roghani, A.; Schliebs, R.; Brust, P.; Sabri, O.; Steinbach, J. *Nucl. Med. Biol.* **2008**, *35*, 185.
34. Kawamura, K.; Ishiwata, K.; Shimada, Y.; Kimura, Y.; Kobayashi, T.; Matsuno, K.; Homma, Y.; Senda, M. *Ann. Nucl. Med.* **2000**, *14*, 285.
35. Kawamura, K.; Ishiwata, K.; Tajima, H.; Ishii, S.-I.; Matsuno, K.; Homma, Y.; Senda, M. *Nucl. Med. Biol.* **2000**, *27*, 255.
36. Matsuno, K.; Nakazawa, M.; Okamoto, K.; Kawashima, Y.; Mita, S. *Eur. J. Pharmacol.* **1996**, *306*, 271.
37. Deuther-Conrad, W.; Maisonial, A.; Patt, M.; Stittsworth, S.; Becker, G.; Habermann, B.; Holl, K.; Schepmann, D.; Funke, U.; Donat, C.; Fischer, S.; Hiller, A.; Wenzel, B.; Jörg, S.; Wünsch, B.; Lever, S. Z.; Hesse, S.; Sabri, O.; Brust, P. *J. Labelled Compd. Rad.* **2013**, *56*, S55.
38. Wong, D. F.; Rosenberg, P. B.; Zhou, Y.; Kumar, A.; Raymont, V.; Ravert, H. T.; Dannals, R. F.; Nandi, A.; Brasic, J. R.; Ye, W. G.; Hilton, J.; Lyketsos, C.; Kung, H. F.; Joshi, A. D.; Skovronsky, D. M.; Pontecorvo, M. J. *J. Nucl. Med.* **2010**, *51*, 913.